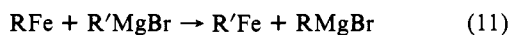


Figure 2. Polarization ratio of isobutyl iodide and isobutylmagnesium bromide as a function of initial concentration ratio of isobutyl iodide and ethylmagnesium bromide.

$$\frac{I_{i\text{-BuI}}}{I_{i\text{-BuMgBr}}} = \frac{k_i T_1 [i\text{-BuI}]}{k_m T_1' [\text{EtMgBr}]}$$

where T_1 , T_1' , and $T_{1,R}$ are the spin-lattice relaxation times of the α -protons of isobutyl iodide, isobutylmagnesium bromide, and isobutyl radical, respectively. Figure 2 shows the relative intensities of these two signals measured 20 s after the introduction of 2.0×10^{-5} M $\text{Fe}(\text{acac})_3$ to 1.6 M ethylmagnesium bromide and 0.2–1.7 M isobutyl iodide. Since these solutions are relatively viscous, we make the approximation that $T_1 = T_1'$,⁸ and find that $k_i/k_m \cong 10^2$. k_m must be $>10^5 \text{ M}^{-1} \text{ s}^{-1}$ to be competitive with $1/T_{1,R}$ and therefore $k_i > 10^7 \text{ M}^{-1} \text{ s}^{-1}$.⁹

It has been suggested that halogen-metal exchange occurs via alkyl iron intermediates formed according to (4) followed by transmetalation with Grignard reagent.^{1,2}



While this mechanism is not ruled out under different conditions, k_4 would have to be $10^{10} \text{ M}^{-1} \text{ s}^{-1}$ (faster than the diffusion-controlled rate in these viscous solutions) to make a significant contribution to exchange at the catalyst concentration used in this study. This suggests that the yield of alkyl dimer formed by radical pair coupling, (5), should be dependent on such reaction parameters as catalyst concentration and overall rate. At the relatively low reaction rates studied by Tamura and Kochi,² the second-order radical termination reaction, (5), may not be significant since the steady-state radical concentration is low. Free radicals may be trapped by reduced iron, alkyl halide, or Grignard reagents via reactions 4, 6, and 7 leading to no observed alkyl dimers. At the higher reaction rates necessary for the observation of CIDNP³ the steady-state radical concentration increases, resulting in a sharp increase in probability of reaction 5 and the observation of dimeric products. Simulations¹⁰ of the concentration profiles of the reactants, intermediates, and products⁵ confirm this hypothesis and indicate that reactions 1–7 are so far sufficient to explain the predominant reaction pathways.

Density Functional Approach to the Frontier-Electron Theory of Chemical Reactivity

Robert G. Parr* and Weitao Yang

Department of Chemistry
University of North Carolina
Chapel Hill, North Carolina 27514

Received February 6, 1984

We here demonstrate that most of the frontier-electron theory of chemical reactivity¹ can be rationalized from the density functional theory of the electronic structure of molecules.^{2,3}

Consider a species S with N electrons, having ground-state electronic energy $E[N, v]$ and chemical potential $\mu[N, v]$, where v is the potential acting on an electron due to all nuclei present. The chemical potential is the negative of the electronegativity.⁴ The energy as a function of N has a discontinuity of slope at each integral N ,⁵ and so there are three distinct chemical potentials for each integral N , $\mu^- = (\partial E / \partial N)_v^-$ (from positive-ion side), $\mu^+ = (\partial E / \partial N)_v^+$ (from negative-ion side), and $\mu^0 = (\partial E / \partial N)_v^0 = 1/2(\mu^+ + \mu^-)$ (unbiased).

Fundamental equations for changes in energy and chemical potential are

$$dE = \mu dN + \int \rho(\vec{r}) dv(\vec{r}) d\vec{r} \quad (1)$$

and

$$d\mu = 2\eta dN + \int f(\vec{r}) dv(\vec{r}) d\vec{r} \quad (2)$$

where $\rho(\vec{r})$ is the electron density, $\eta = 1/2(\partial\mu/\partial N)_v$ is the hardness,⁶ and the function $f(\vec{r})$ is defined by

$$f(\vec{r}) \equiv [\delta\mu/\delta v(\vec{r})]_N = [\partial\rho(\vec{r})/\partial N]_v \quad (3)$$

The equality in this formula is a Maxwell relation for eq 1.⁷ The function f is a local quantity, which has different values at different points in the species. It admits of contour maps.

Our argument will be that large values of f at a site favor reactivity of that site. We therefore call $f(\vec{r})$ the *frontier function* or *fukui function* for a molecule.

If a reagent R approaches S , what direction will be preferred (from among several directions that can produce the same type of chemical bond)? The quantity $d\mu$ in eq 2 measures the extent of the reaction. We assume that the preferred direction is the one for which the initial $|d\mu|$ for the species S is a maximum. The first term on the right side of eq 2 involves only global quantities and at large distances is ordinarily less direction sensitive than the second term. We may then assume, more or less equivalently in the usual cases, that the preferred direction is the one with largest $f(\vec{r})$ at the reaction site. Reactivity is measured by the fukui index of eq 3.

Equation 3 in fact provides three reaction indices, because $\rho(\vec{r})$ as a function of N , like $E(N)$, has slope discontinuities.⁵ We therefore have the firm predictions, governing electrophilic attack,

$$f^-(\vec{r}) = [\partial\rho(\vec{r})/\partial N]_v^- \quad (4)$$

governing nucleophilic attack,

$$f^+(\vec{r}) = [\partial\rho(\vec{r})/\partial N]_v^+ \quad (5)$$

and governing neutral (radical) attack,

(1) Fukui, K. "Theory of Orientation and Stereoselection"; Springer-Verlag: Berlin, 1973; p 134; *Science (Washington, D. C.)* **1982**, *218*, 747–784.

(2) Hohenberg, P.; Kohn, W. *Phys. Rev.* **1964**, *136*, B864–B871.

(3) Parr, R. G. *Annu. Rev. Phys. Chem.* **1983**, *34*, 631–656.

(4) Parr, R. G.; Donnelly, R. A.; Levy, M.; Palke, W. E. *J. Chem. Phys.* **1978**, *68*, 3801–3807.

(5) Perdew, J. P.; Parr, R. G.; Levy, M.; Balduz, J. L., Jr. *Phys. Rev. Lett.* **1982**, *49*, 1691–1694.

(6) Parr, R. G.; Pearson, R. G. *J. Am. Chem. Soc.* **1983**, *105*, 7512–7516.

(7) Nalewajski, R.; Parr, R. G. *J. Chem. Phys.* **1982**, *77*, 399–407.

(7) Lehr, G. F. Ph.D. Thesis, Brown University, Providence, RI, 1981.

(8) Carrington, A.; McLachlan, A. D. "Introduction to Magnetic Resonance"; Wiley: New York, 1967; pp 176–203.

(9) Cooper, R. A.; Lawler, R. G.; Ward, H. R. *J. Am. Chem. Soc.* **1972**, *94*, 545.

(10) Stabler, R. N.; Chesick, J. *Int. J. Chem. Kinet.* **1978**, *10*, 461.

$$f^0(\vec{r}) = [\partial\rho(\vec{r})/\partial N]_0^0 \quad (6)$$

The three cases have $\mu_S > \mu_R$, $\mu_S < \mu_R$, and $\mu_S \sim \mu_R$. A "frozen core" approximation now gives $d\rho = d\rho_{\text{valence}}$ in each case, and therefore, governing electrophilic attack,

$$f^-(\vec{r}) \approx \rho_{\text{HOMO}}(\vec{r}) \quad (7)$$

governing nucleophilic attack,

$$f^+(\vec{r}) \approx \rho_{\text{LUMO}}(\vec{r}) \quad (8)$$

and governing radical attack,

$$f^0(\vec{r}) \approx \frac{1}{2}[\rho_{\text{HOMO}}(\vec{r}) + \rho_{\text{LUMO}}(\vec{r})] \quad (9)$$

These are the rules of classical frontier theory.¹ Errors in eq 7-9 should be small in the outer reaches of the species toward which the reagent approaches.

Frontier theory is equivalent, then, to the assumption that it is favorable for f to be big at a site, or that direction is preferred along which the incoming reagent will produce the biggest change in the system's electronic chemical potential.

Acknowledgment. Research grants from the National Institutes of Health and the National Science Foundation are gratefully acknowledged.

Trigonal-Bipyramidal Methyl Group Bridging Two Zirconocene-Ketene Centers

Robert M. Waymouth, Bernard D. Santarsiero, and Robert H. Grubbs*

Contribution No. 6996, Laboratories of Chemistry
California Institute of Technology
Pasadena, California 91125
Received March 5, 1984

The role of methyl groups as bridging ligands has been a central topic in organometallic chemistry.¹ Although there was early controversy concerning the exact structure of such bridging groups,² it is well established that methyl bridges play a key role in alkylaluminum chemistry. In these cases and in most transition-metal analogues, the M-C-M angle is less than 90°. Only recently have complexes in which this angle approaches 180° been considered.³⁻⁵ Calculations on Li_2CH_3^+ suggest that the linear M-C-M geometry is the most stable.³ A neutron diffraction study of a B-CH₃Li complex indicated a linear structure in which the sp³-methyl hydrogen atoms bridged to the lithium.⁴ A linear methyl bridge has been reported for the dimer of a bis(pentamethylcyclopentadienyl)lutetium methyl complex.^{5a} We report here the preparation of a complex in which a near-planar methyl group bridges two zirconium atoms.

In an attempt to activate zirconocene ketene complexes, a toluene solution of complex I⁶ was treated with 1 equiv of tri-

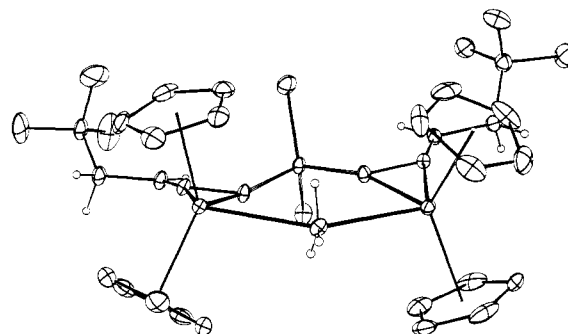
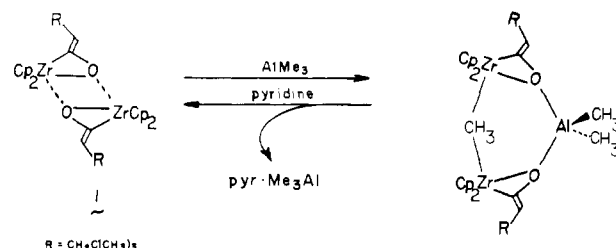


Figure 1. ORTEP diagram of II. Hydrogens on the cyclopentadienyl, *tert*-butyl, and aluminum methyl groups have been omitted for clarity.

Scheme I



R = CH₂C(CH₃)₃

methylaluminum. An intermediate forms and is observed to rearrange quantitatively to a symmetrical complex, II (Scheme I).⁷ Colorless crystals of II suitable for an X-ray structure determination were obtained in 55% yield from a toluene-pentane solution.⁸ The molecular structure of II is shown in Figure 1, and relevant bond angles and lengths are given in Figure 2. The bridging methyl hydrogens were located from a difference map and refined to a final $R = 0.081$ and a goodness-of-fit = 1.63 when averaged over 6573 reflections.

From the crystal structure, it is clear that the bridging methyl group is very nearly planar, approaching a trigonal-bipyramidal configuration. The carbon atom is displaced 0.08 Å out of the hydrogen atom plane; for a typical sp³-hybridized methyl group, the carbon atom is displaced 0.3 Å out of the hydrogen atom plane. From Figure 2, it is also evident that the methyl bridge is not symmetrical but is 0.1 Å closer to Zr(2) than to Zr(1). This is

(7) II: ¹H NMR (benzene-*d*₆) δ 6.05 (t, ³J_{HH} = 7.3 Hz, 2H), 5.64 (s, 20 H), 2.14 (d, ³J_{HH} = 7.3 Hz, 4 H), 1.14 (s, 18 H), -0.19 (s, 3 H), -0.46 (s, 6 H); ¹³C NMR (benzene-*d*₆) δ 178.3 (d, ²J_{CH} = 7.3 Hz, CO), 107.0 (d, ¹J_{CH} = 171.3 Hz, C₅H₅), 102.1 (d, ¹J_{CH} = 147.9 Hz, CH), 44.9 (t, ¹H_{CH} = 123.7 Hz, CH₂), 31.6 [s, C(CH₃)₃], 30.0 [q, ¹J_{CH} = 124.5 Hz, C(CH₃)₃], -9.24 (q, ¹J_{CH} = 136.2 Hz, CH₃).

(8) II: crystal data, space group $P2_1/c$ ($0k0$ absent for k odd, $h0l$ absent for l odd); the unit cell parameters [$a = 10.2089$ (7) Å, $b = 20.214$ (3) Å, $c = 18.421$ (2) Å, $\beta = 94.375$ (8)°, $V = 3790.4$ (7) Å³, $Z = 4$] were obtained by least-squares refinement of 25 2θ values. The data were collected at room temperature on a crystal mounted approximately along c in a glass capillary under N₂ with an Enraf-Nonius CAD4 diffractometer (graphite monochromator and Mo K α radiation $\lambda = 0.71073$ Å). The total, 10 114 ($+h, \pm k, \pm l$), yielded an averaged data set of 6573 reflections upon deletion of 87 for overlap; 5216 had $I > 0$ and 3380 had $I > 3\sigma(I)$. The four check reflections indicated no decomposition, and the intensity data were reduced to F^2 . The positions of the two independent Zr atoms were derived from the Patterson map, and the subsequent Fourier map phased on these two atoms revealed the remainder of the structure. The bridging methyl hydrogen atoms and those on the *tert*-butyl groups were located from difference maps; all other hydrogen atoms were introduced into the model at idealized positions with isotropic $U = 0.101$ Å². Least-squares refinement of atomic coordinates and U 's [anisotropic for all nonhydrogen atoms and isotropic for H(1), H(2), and H(3)] minimizing $\sum w\Delta^2$ with weights $w = \sigma^{-2}(F_o^2)$ and $\Delta = F_o^2 - (F_c/k)^0$ gave $R_F = \sum ||F_o| - |F_c|| / \sum |F_o| = 0.0813$ [for $I > 0$, $R_F = 0.042$ for $I > 3\sigma(I)$] and S (goodness-of-fit) = $[\sum w\Delta^2 / (n-p)]^{1/2} = 1.63$ ($p = 391$ parameters); and the maximum shift/error ratio is 0.50, the average <0.10, and the maximum deviations in the $\Delta\rho$ map are close to the Zr atoms and are less than 1.1 e Å⁻³. All calculations were carried out on a VAX 11/780 computer using the CRYRM system of programs. The form factors for all atoms were taken from *Int. Tables X-Ray Crystallogr.* (1974), Table 2.2B. Those for Zr and Al were corrected for anomalous dispersion.

(1) Holton, J.; Lappert, M. F.; Pearce, R.; Yarrow, P. I. W. *Chem. Rev.* 1983, 83, 135.

(2) Huffman, J. C.; Streib, W. E. *J. Chem. Soc. D* 1971, 911.

(3) (a) Jemmis, E. D.; Chandrasekhar, J.; Schleyer, P. v. R. *J. Am. Chem. Soc.* 1979, 101, 527. (b) Schleyer, P. v. R.; Tidor, B.; Jemmis, E. D.; Chandrasekhar, J.; Wurthwein, E. U.; Kos, A. J.; Luke, B. T.; Pople, J. A. *Ibid.* 1983, 105, 484. (c) See also: Chinn, Jr., J. W.; Lagow, R. J. *Organometallics* 1984, 3, 75.

(4) (a) Rhine, W. E.; Stucky, G.; Peterson, S. W. *J. Am. Chem. Soc.* 1975, 97, 6401. (b) Groves, D.; Rhine, W.; Stucky, G. D. *Ibid.* 1971, 93, 1553.

(5) (a) Watson, P. L. *J. Am. Chem. Soc.* 1983, 105, 6491. (b) Forbus, T. R.; Martin, J. C. *Ibid.* 1979, 101, 5057. (c) Engelhardt, L. M.; Leung, W.; Raston, C. L.; Twiss, P.; White, A. H. *J. Chem. Soc., Dalton Trans.* 1984, 321. (d) Kaminsky, W.; Kopf, J.; Sinn, H.; Vollmer, H. *J. Angew. Chem., Intl. Ed. Engl.* 1976, 15, 629.

(6) (a) Straus, D. A.; Grubbs, R. H. *J. Am. Chem. Soc.* 1982, 104, 5499. (b) Straus, D. A. Ph.D. Thesis, California Institute of Technology, Pasadena, CA 1982. (c) Ho, S. C. H.; Straus, D. A.; Armantrout, J.; Schaefer, W. P.; Grubbs, R. H. *Ibid.* 1984, 106, 2210. (d) Moore, E. J.; Straus, D. A.; Armantrout, J.; Santarsiero, B. D.; Grubbs, R. H.; Bercaw, J. E. *Ibid.* 1983, 105, 2068.